Sounding of the plasmasphere by Mid-continent MAgnetoseismic Chain (McMAC) magnetometers

P. J. Chi,[1] M. J. Engebretson,[2] M. B. Moldwin,[3] C. T. Russell,[1] I. R. Mann,[4] M. R. Hairston,[5] M. Reno,[6] J. Goldstein,[7] L. I. Winkler,[8] J. L. Cruz-Abeyro,[9] D.-H. Lee,[10] K. Yumoto,[11] R. Dalrymple,[12] B. Chen,[13] and J. P. Gibson[14]

Received 6 September 2012; revised 8 April 2013; accepted 10 April 2013; published 14 June 2013.

[1] We present a statistical analysis on the plasmaspheric mass density derived from the field line resonance (FLR) observations by the Mid-continent MAgnetoseismic Chain (McMAC). McMAC consists of nine stations in the United States and Mexico along the 330° magnetic longitude, spanning L-values between 1.5 and 3.4. Using the gradient method and an automated procedure for FLR detection, we studied a full year of McMAC observations between July 2006 and June 2007. We find that the rate of FLR detection can reach as high as 56% around local noon at $L = 2.7$, and the detection rates at higher and lower L-values decline due to the occasional presence of the plasmapause and weaker FLR signals, respectively. At L-values between 1.8 and 3.1, the inferred equatorial plasma mass density follows the L-dependence of L^{-4}. By comparing the mass density with the electron density, we found that the ion mass gradually decreased from 1.7 amu at $L = 1.8$ to 1 amu at $L = 3.1$. The plasma mass density exhibits an annual variation that maximizes in January, and at $L = 2.4$ the ratio between January and July densities is 1.6. Our observations also show a local time dependence of plasmaspheric mass density that stays steady in the morning and rises postnoon, a phenomenon that may be attributed to the equatorial ionization anomaly as a part of the plasma neutral coupling at low latitude.

Citation: Chi, P. J., et al. (2013), Sounding of the plasmasphere by Mid-continent MAgnetoseismic Chain (McMAC) magnetometers, *J. Geophys. Res. Space Physics*, *118*, 3077–3086, doi:10.1002/jgra.50274.

1. Introduction

[2] The understanding of plasma density variations in the magnetosphere can help predict space weather and its effects on space systems. For instance, particle heating and instability growth rates can be strongly influenced by the presence and concentrations of low-energy core plasmas. Spacecraft charging and the resulting risk of damaging spacecraft electronics can also be mitigated by core plasma. Furthermore, an accurate density model is needed by the numerical modeling of global magnetospheric properties and processes in a realistic environment.

[3] Inferring the plasma mass density in the magnetosphere through ground-based observations of field line resonance (FLR) frequencies started in the early years of space physics [*Obayashi and Jacobs*, 1958]. In the 1970s more accurate determination of FLR in ground data was performed by identifying the phase reversal across the resonance latitude [see, for example, *Webb et al*., 1977], following the phase variation in the FLR theory as predicted by *Tamao* [1966], *Chen and Hasegawa* [1974], and *Southwood* [1974]. After *Baransky et al*. [1985] developed the concept of FLR detection in ground data and *Waters et al*. [1991] obtained successful results with

[1]Institute of Geophysics and Planetary Physics and Department of Earth and Space Sciences, University of California, Los Angeles, California, USA.
[2]Department of Physics, Augsburg College, Minneapolis, Minnesota, USA.
[3]Department of Atmospheric, Oceanic and Space Sciences, University of Michigan, Ann Arbor, Michigan, USA.
[4]Department of Physics, University of Alberta, Edmonton, Alberta, Canada.
[5]William B. Hanson Center for Space Sciences, University of Texas Dallas, Richardson, Texas, USA.
[6]Austin Mission Consulting, Austin, Texas, USA.
[7]Department of Space Sciences, Southwest Research Institute, San Antonio, Texas, USA.
[8]Department of Physics and Astronomy, Minnesota State University Moorhead, Moorhead, Minnesota, USA.
[9]Centro de Geociencias, Universidad Nacional Autónoma de México, Juriquilla, Querétaro, Mexico.
[10]School of Space Research, Kyung Hee University, Yongin, Gyeonggi, Korea.
[11]International Center for Space Weather Science and Education, Kyushu University, Fukuoka, Japan.
[12]Minnesota West Community and Technical College, Worthington, Minnesota, USA.
[13]Department of Computer and Electronics Engineering, University of Nebraska-Lincoln, Omaha, Nebraska, USA.
[14]Kessler Atmospheric and Ecological Field Station, University of Oklahoma, Norman, Oklahoma, USA.

Corresponding author: P. J. Chi, University of California, Los Angeles, IGPP/UCLA, Box 951567, Los Angeles, CA 90095–1567, USA. (pchi@igpp.ucla.edu)

2169-9380/13/10.1002/jgra.50274

modified techniques, ground-based observations of FLR have opened up a new window of estimating the plasma density in the magnetosphere. The inferred density from FLR is unique as it represents the mass density in the magnetosphere, containing contributions not only from H^+ but also from heavy ions.

[4] Since the 1990s dozens of studies have made use of the FLR method to study ground-based magnetic field observations for investigation of the characteristics of the inferred magnetospheric mass density. For example, *Vellante and Förster* [2006] examined the consistency between the plasma mass density model and FLR frequencies, *Berube et al*. [2005] used FLR observations to develop models of plasmasphere density, and *Vellante et al*. [2007] identified how the solar radiation controls the FLR frequencies/inferred density. Some other studies demonstrated the capability of using FLR observations to monitor the plasmapause motion [e.g., *Menk et al*., 1999, 2004; *Milling et al*., 2001]. The comparison between the FLR-inferred mass density and space-borne observations, including the EUV images of the plasmasphere and plasma density derived from wave experiments, has shown good agreement in terms of the region of measurement [e.g., *Dent et al*., 2003; *Grew et al*., 2007; *Obana et al*., 2010]. A subject of interest to many is the response of plasma mass density during magnetic storms, and studies have shown that the plasmasphere can undergo significant depletion or density enhancement due to the interaction with the disturbed ionosphere [*Chi et al*., 2000, 2005; *Vellante et al*., 2002; *Dent et al*., 2006].

[5] As the technique of FLR sounding becomes mature, statistical studies that can provide overall characteristics of the inferred plasma mass density are still rare and limited in spatial coverage. The insufficiency of statistical studies on FLR sounding is mainly due to the technical reality that the identification of FLR signatures in data has mostly been performed by visual inspection. Statistical analysis on a large data set can be made possible only through automatic FLR identification, allowing us to be certain about the empirical behaviors of density variations in response to different solar and geomagnetic conditions.

[6] In this paper, we present the results of FLR sounding based on the first year of observations by the Mid-continent MAgnetoseismic Chain (McMAC). We developed an automated program for FLR detection in McMAC observations and built a database of fundamental mode frequencies for L-values ranging from 1.6 to 3.3. With this database we analyzed the statistical trends of the inferred plasmaspheric mass density. The results show that the equatorial mass density of the plasmasphere has an L-dependence of L^{-4} and an annual variation similar to those in ionospheric and thermospheric densities. We also analyzed the local time distribution of plasmaspheric mass density, and the results show a rise in density in afternoon hours for all the latitudes studied and further density increases in evening hours between 2 and 3 in L-values.

[7] In the following section, we describe the construction of McMAC magnetometers and the site selection. Section 3 introduces examples of the FLR observations by McMAC and how our automated algorithm identifies FLR signatures from a full year of data. Section 4 describes the statistical results of the inferred plasmaspheric mass density, including its dependence of the L-value, the local time distribution, and the annual variation. We conclude by discussing the results consistent with our previous understanding, as well as those that are unexpected.

2. Mid-continent MAgnetoseismic Chain

[8] In addition to providing the observations for composing geomagnetic indices and inferring electric currents in the ionosphere and the magnetosphere, suitably located ground-based magnetometers can be used to monitor the mass density of magnetospheric plasma through the observations of field line resonance. The resonant frequency depends on the magnetic field strength and mass density along the field line. Because the magnetic field is well modeled, especially in inner L-shells, the mass density can be inferred by the observed resonant frequency provided that a reasonable field-aligned density distribution is assumed. The frequency of FLR depends most strongly on the mass density in the equatorial region where wave velocity is the lowest [e.g., *Dungey*, 1954], making the estimate of equatorial mass density vary more weakly with changes in the assumed field-aligned density distribution.

[9] The pulsation spectrum, however, is inevitably composed of contributions from both driving waves and resonating waves [*Kurchashov et al*., 1987], and in many instances the upstream waves in the foreshock region [e.g., *Troitskaya*, 1994; *Chi et al*., 1994] and the Kelvin-Helmholtz instability on the magnetopause [e.g., *Samson*, 1972] constitute a significant portion of wave energy. The difficulty in distinguishing the resonant wave from the driving wave was resolved by *Baransky et al*. [1985] and *Kurchashov et al*. [1987] who devised the so-called "gradient method" that makes use of the observations by two ground-based magnetometers located on the same longitude but closely separated in latitude. By comparing either the amplitude or phase of the wave signals at the two observatories, one can filter out the source signals and thus identify the characteristics of resonant waves.

[10] Following the simple profile of a resonant wave [e.g., *Pilipenko and Fedorov*, 1994] under the typical magnetospheric condition when the Alfvén velocity slowly decreases with latitude, Figure 1 depicts the phase differences and amplitude ratios expected in the observations by a pair of ground stations. Similar diagrams have appeared in several previous studies, such as *Baransky et al*. [1985], *Waters et al*. [1991], and *Kawano et al*. [2002]. The left panel shows the latitudinal profile of amplitude and phase for three different frequencies. For each frequency the phase undergoes a transition centered at the resonance point by close to 180°. If two ground stations at different latitudes are located close to the resonant location, a noticeable difference in phase can be observed by the two stations, and the phase difference as a function of frequency maximizes at the frequency associated with the resonant field line midway between the two stations. The amplitude ratio as a function of frequency also experiences a transition across the resonant frequency from minimum to maximum. It is possible to use either the observation of phase differences or that of amplitude ratios to identify FLR frequencies, and *Russell et al*. [1999] provided a comparison between the two approaches as well as the technique using the H/D ratio

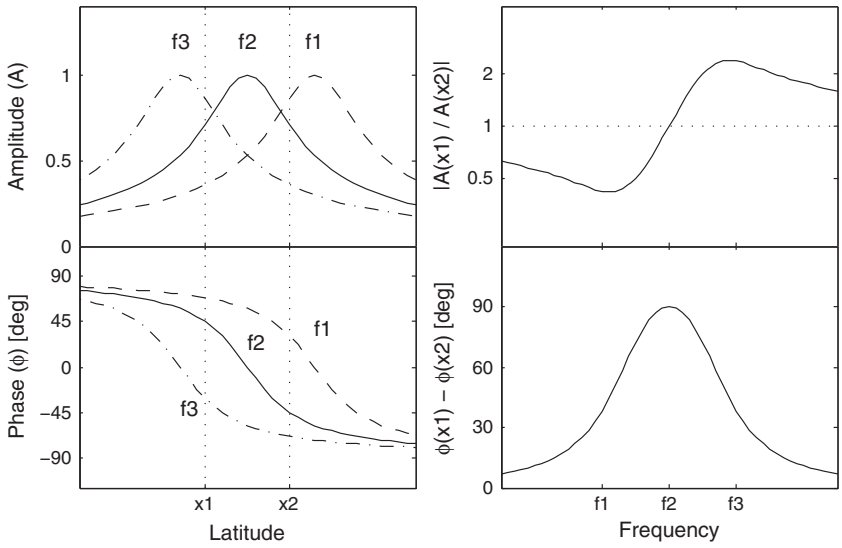

Figure 1. (left) Amplitude and phase for field line resonance oscillations as functions of latitude. (right) Amplitude ratio and phase difference that are expected to be observed by two stations located at different latitude.

observed by a single station. In the region near the plasmapause or in the topside ionosphere the Alfvén speed can increase with latitude, the phase function in Figure 1 switches signs and the phase differences become negative [see, for example, *Waters*, 2000; *Kawano et al*., 2002].

[11] The nine McMAC magnetometer stations were established to make use of the above principles of FLR sounding to systematically observe the variations of plasmaspheric density from the ground. Figure 2 and Table 1 show the locations of the McMAC stations and the Cambridge station previously installed as a part of the IGPP-LANL magnetometer array. The McMAC stations are placed as close to the 330° magnetic longitude as possible. The major motivation is that this is the meridian in the world where land covers the greatest continuous range in magnetic latitude. Observations at the same local time do not suffer from the possible azimuthal phase differences that could result from the separation in the east-west direction. Along this meridian the "Churchill Line" of CARISMA magnetometers have been established to provide coverage in central Canada. Between the U.S.-Canada border and the Pacific Ocean on this meridian there is still land stretching more than 3000 km for possible implementation of ground-based magnetometers. In light of previous studies suggesting that the maximum spacing between stations for effective use of the gradient method should be below 540 km [*Menk et al*., 1999], the locations of McMAC stations were chosen so that the average separation between adjacent stations is 272 km. The local time of the chain is approximately 6.5 h behind Universal Time (UT).

[12] Each McMAC station is equipped with a three-component fluxgate magnetometer that has an identical design to those developed for the THEMIS ground-based magnetometers [*Russell et al*., 2008]. The sensors are connected to a 22-bit analog-to-digital converter in a low-noise electronic environment, and the magnetic field vectors are returned with a digitization resolution of 9.5 pT. During the installation the magnetometer determines the offset currents in the three components to compensate the background magnetic field, and the field fluctuations are measured with a dynamic range of 5000 nT. The noise floor is $\cong 10^{-3}$ nT^2 / Hz, and the data are sampled at 2 Hz, allowing studies of magnetic fluctuations with frequencies ranging from DC to 1 Hz. Also included in the magnetometer system are a PC for data acquisition and storage, a GPS antenna for accurate timing, and a small battery for mitigating power brownouts. At all McMAC stations the magnetometer system is connected to the Internet and can transmit data to the data center at UCLA for monitoring the operation.

3. Data

[13] The McMAC stations along the same longitude have been able to reveal in detail the latitudinal structure of ULF

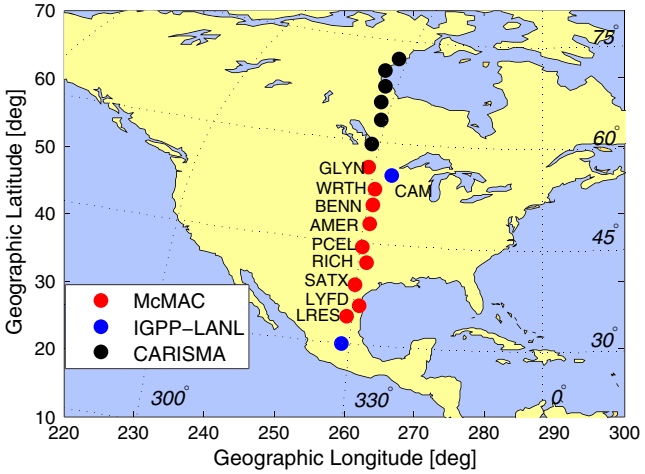

Figure 2. Map of McMAC and ground-based magnetometer stations along the same magnetic meridian. The 10 stations whose data are examined in this study are labeled.

Table 1. Names and Locations of the Ten Magnetometer Stations Included in This Study

Station Name	Station Code	Geographic Longitude	Geographic Latitude	*L*
Glyndon	GLYN	263.55	46.87	3.42
Cambridge[a]	CAM	266.75	45.56	3.18
Worthington	WRTH	264.4	43.6	2.86
Bennington	BENN	263.84	41.36	2.58
Americus	AMER	263.7	38.5	2.28
Purcell	PCEL	262.6	35.0	1.99
Richardson	RICH	263.25	32.98	1.87
San Antonio	SATX	261.39	29.44	1.66
Lyford	LYFD	262.2	26.4	1.53
Linares	LRES	260.4	24.8	1.46

[a]The Cambridge, MN station was established by the IGPP-LANL magnetometer array.

waves at low magnetic latitudes. The left plot in Figure 3 presents an example of the McMAC observations in the *H* component for a period of one day when no major geomagnetic activity was present. In the Figure the baseline of *H* for each station is adjusted so that all the observations can fit into the same plot. For the time scales discernible in this daily magnetogram, magnetic fluctuations are almost identical across all McMAC stations at *L*-values between 1.53 and 3.42. By comparing with the solar wind data on the same day (not shown), we found that some of the magnetic fluctuations appeared to associate with changes in the solar wind. For example, the spike in the *H* component at about 0400 UT coincides with the doubling of the solar wind proton density. The right plot in Figure 3 focuses on the 15 min of observations at 1945–2000 UT (or equivalently 1315–1330 LT) on the same day. In this zoom-in plot Pc 3–4 waves were observed by all McMAC stations. Unlike the fluctuations on longer time scales, however, the frequency and phase of the Pc 3–4 waves can vary within the limited range of magnetic latitude covered, an expected result when the latitude-dependent field line resonance is present in the observed region.

[14] As summarized in the previous section, the gradient method is a powerful technique to detect FLR frequencies with a pair of well-positioned magnetometer stations. Figure 4 shows an example of FLR detection using the measurements from the McMAC Worthington and Bennington stations during 31 July 2006. The colors in the Figure represent the phase differences observed between the two stations, and this so-called "cross-phase spectrogram" is an effective way to reveal FLR frequencies where phase differences are expected to peak (cf. Figure 1). In Figure 4 the majority of large phase differences appear on the right side of the spectrogram, which in most part corresponds to daytime hours. The gradient method also examines other properties of the cross-spectrum, such as the coherence and amplitude ratio, to determine if the result is in fact consistent with an FLR signature.

[15] Because identifying FLR frequencies in a large amount of data is very time-consuming, we have developed a computer program that automates the process. The basic elements in the gradient analysis are the power spectral density for the observation at each station and the cross-spectra, including the phase and coherence, between the stations. Using the Fast Fourier transform, we calculated these values for each time window of 2048 s and advanced 600 s for each time step. We also examined the statistics of the values within a time-frequency box that spans 5 points in time (i.e., 50 min) and 7 points in frequency (i.e., 3.4 mHz) before determining if the results are consistent with a FLR signature. The selection criteria for FLR frequencies include: (1) It is a peak in the phase-difference spectrum; (2) The *t*-statistic, i.e., the local average divided by the local deviation, of phase differences in the time-frequency box is no less than one. This *t*-statistic is a useful measure for the significance of a peak. (3) The coherence is no less than 0.5. (4) The amplitude ratio at the frequency has a positive

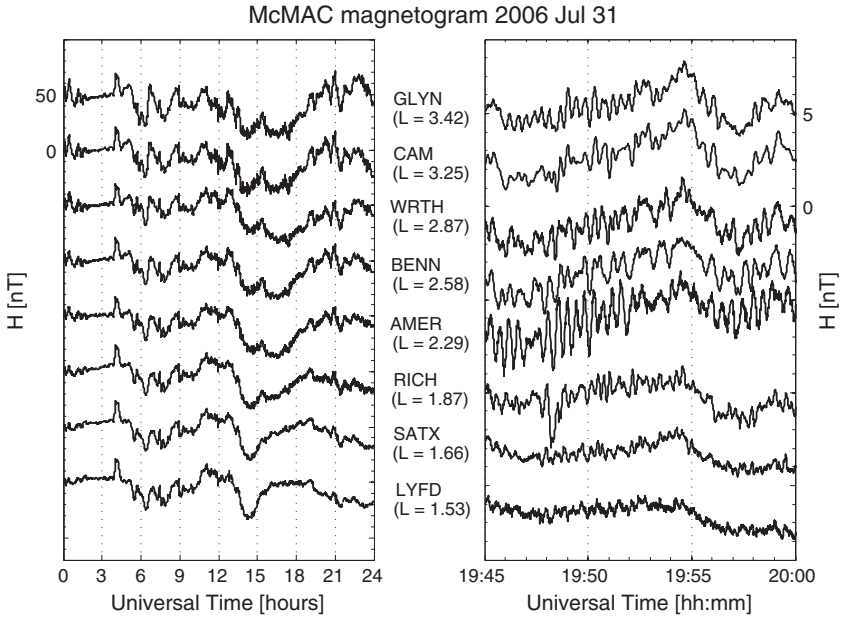

Figure 3. (left) Magnetic variations in the *H*-component from eight stations along 330° magnetic longitude for the day of 31 July 2006. (right) A close-up of the magnetic variations during 1945–2000 UT reveals Pc 3–4 waves with details that vary from station to station.

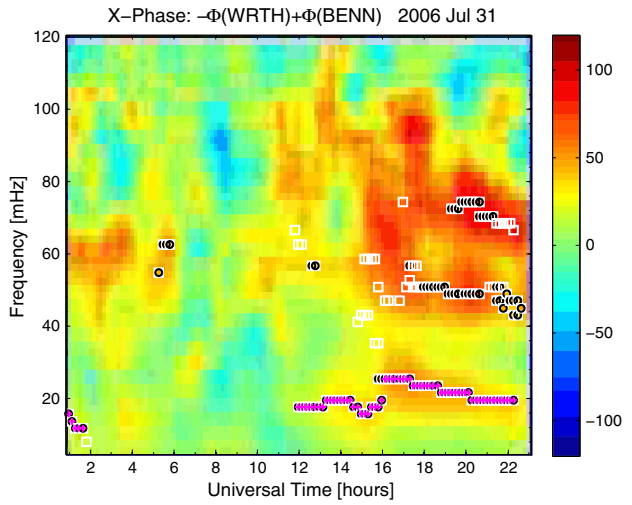

Figure 4. Cross-phase spectrogram for the joint observation by two McMAC magnetometers in Worthington and Bennington. Colors represent the phase differences in degrees. Magenta circles denote the fundamental mode frequencies selected by automated FLR identification. See paper for detailed description about what other symbols represent.

slope. These criteria are in principle consistent with those used by *Berube et al*. [2003] except that we added Criterion (3) on the minimum coherence to ensure that sufficient power of coherent signals was seen by both stations. As we focus on the fundamental mode frequency in this study, we also devised the following additional features in our algorithm for automatic FLR identification: (5) The program makes the selection without the need to specify the possible frequency range. (6) The selected frequency needs to vary less than 3 mHz per 10 min and to persist for at least 30 minutes. An example of FLR identification is shown in Figure 4, where white squares represent the initial selection of frequencies using Criteria (1), (2), and (3), and black circles are those that also satisfy Criterion (4). The magenta crosses denote the FLR frequencies that satisfy all the six criteria, and in this example the fundamental mode frequency varied between 12 and 26 mHz during the day. The gradual decline in FLR frequency in afternoon hours is a phenomenon often seen in McMAC observations, and we will return to this point later.

[16] We studied a full year of data collected during July 2006 to July 2007 when all the ten stations listed in Table 1 operated for more than 80% of the time over one consecutive year. The ten magnetometer stations form nine pairs of neighboring stations, and Table 2 lists the *L*-values of their midpoint locations. Depending on the station pair, the selection criteria we used identified up to 2051 h of positive FLR detection in a year of observations. Figure 5 shows, for each 1 h bin in UT, the ratio of the number of hours with FLR detection divided by the total hours of observations. Hereafter, we refer to this ratio as the rate of FLR detection. The *L*-value noted for each distribution is associated with the midpoint of the station pair. We excluded the result for the Lyford-Linares pair at $L = 1.5$ because its maximum FLR detection rate was merely 0.6%. We should note here that the rate of FLR detection can be influenced by many factors, including the occurrence of FLR in the magnetosphere, wave amplitude of FLR, the distance between the two stations, and the criteria used in FLR selection. Specifically, the selection criteria used in this study may miss the FLR occurring within the plasmaspheric boundary layer where the phase difference can be negative.

[17] Of all the nine station pairs, the Bennington-Americus pair at $L = 2.4$ observed most FLR events, for which the maximum detection rate reached 56% at around noon. The next two station pairs toward higher latitudes ($L = 2.7$ and 3.1) observed slightly less FLR events, but at noon the detection rates can still reach approximately 45%. The detection rate observed by the Glyndon-Cambridge pair at $L = 3.3$, on the other hand, drops significantly, and its peak hour shifts to approximately 1530 UT (or 0900 in local time). We believe that the reduced FLR detection at $L = 3.3$ is due to the increased likelihood of the presence of the plasmapause (see section 4 for details). The station pairs at *L*-values lower than 2.4 also observed fewer FLR events, and we consider that the lower FLR detectability at lower latitudes is in part due to the reduced wave amplitude, as exemplified by Figure 3. We note that the rates of FLR detection shown in Figure 5 are lower than those reported by earlier studies. Studying the observations from two magnetometers at $L \sim 1.7$, *Berube et al*. [2003] found FLR signatures in 243 of 341 days (71%). Since they studied the data during 2000–2001, the higher rate of FLR detection might partly be helped by the stronger magnetic fluctuations at solar maximum. In an earlier study by *Waters et al*. [1994] who visually inspected 21 consecutive days of data in October and November 1990, the authors reported that FLR was observed almost every day at $L = 1.8$ and 2.8. We think that the lower FLR detection rates we obtained are likely associated with our coherence criterion for automatic selection, and weak FLR amplitude observed by either station can lead to low coherence and be rejected by the selection process.

4. FLR Frequency and Inferred Plasma Mass Density

[18] Figure 6 presents the histograms of the fundamental mode FLR frequencies (f_1) observed by eight station pairs over a period of one year. For the region between the ionosphere and the plasmapause, the FLR frequency at the peak of distribution shifts toward higher values with decreasing *L*-values of observation, as expected. The f_1 observed by the Glyndon-Cambridge pair at $L = 3.3$ contains not only a group of lower frequencies centered at 7 mHz but also a group of higher frequencies centered at 37 mHz. The

Table 2. Pairs of Neighboring Stations and the *L*-values of Midpoints

Station Pair	*L*
Glyndon – Cambridge	3.3
Cambridge – Worthington	3.1
Worthington – Bennington	2.7
Bennington – Americus	2.4
Americus – Purcell	2.1
Purcell – Richardson	1.9
Richardson – San Antonio	1.8
San Antonio – Lyford	1.6
Lyford - Linares	1.5

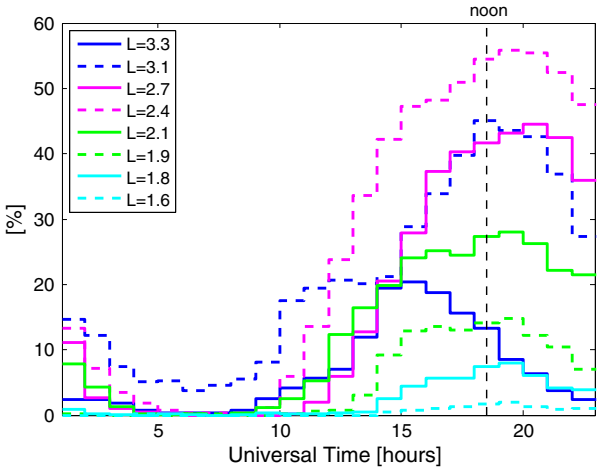

Figure 5. Normalized distribution of FLR detection observed by station pairs at different *L*-values.

higher-frequency group implies an equatorial mass density of 72 amu/cm^3, a value too low for plasmaspheric density but reasonable for plasmatrough density. For example, if we extend the plasmatrough component of the *Carpenter and Anderson* [1992] density model inward to $L = 3.3$, the predicted equatorial density is about 74 el/cm^3.

[19] The observations of f_1 shown in Figure 6 can be translated to plasma mass densities for the associated *L*-shells. In this study we focus on the plasma density distribution inside the plasmasphere and exclude the observations at $L = 3.3$ because many of them were made in the plasmatrough. We also exclude the results at $L = 1.5$ and 1.6 due to low event counts. The principles for estimating density were described by *Cummings et al*. [1969], assuming that (1) the background magnetospheric field lines are dipolar; (2) the plasma mass density varies along the field line as $\rho \propto r^{-m}$; (3) the oscillation propagates as a noncompressional Alfvén wave along the magnetic field line of interest and undergoes a perfect reflection from the ionosphere. We used $m = 1$ for the field-aligned density distribution to be in agreement with the findings by *Takahashi et al*. [2004] and by *Vellante and Förster* [2006]. The function $\rho \propto r^{-m}$ cannot well model the sharp density at ionospheric heights and the region immediately above, but we note that estimation of plasma mass density from FLR places a much heavier weight on the region near the equatorial plane because the Alfvén wave spends most of the travel time there [e.g., *Denton and Gallagher*, 2000]. The upper panel in Figure 7 shows the mean values (in open diamonds) of the estimated equatorial mass density (ρ_m) at *L*-values between 1.8 and 3.1, and the associated standard deviations indicated by error bars. The *L*-dependence of ρ_m well follows L^{-4} indicated by a dashed curve, a dependence inversely proportional to the flux tube volume.

[20] An important aspect of the mass density is that it provides the opportunity to compare against the electron density and assess the significance of heavy ions in the plasma. As our FLR-inferred mass densities are statistical results based on one year of observations, we examine the empirical model of electron density for comparison. The open circles in the upper panel of Figure 7 show the equatorial electron density in the plasmasphere as modeled by *Ozhogin et al*. [2012], and the error bars indicate the standard deviations of model values. The *Ozhogin et al*. [2012] model is to date the most comprehensive plasmasphere model based on IMAGE RPI observations [*Reinisch et al*., 2000], and the model was built upon more than 700 density profiles derived from active sounding measurements between June 2000 and July 2005. As shown by *Ozhogin et al*. [2012], this new model delineates a radial profile of equatorial electron density that is close to the average values between other plasmasphere models [*Carpenter and Anderson*, 1992; *Gallagher et al*., 2000; *Sheeley et al*., 2001; *Denton et al*., 2006], and one of the advantages of this model is its coverage at low *L*-values down to 1.6. The electron density has values that are equal to or lower than those of the mass density, but its fall-off rate with respect to *L* is slightly lower. The comparison between the two densities yields the average ion mass (M_i) plotted in the bottom panel of Figure 7. The value of M_i at $L = 3.1$ is approximately the same as the proton mass, and it gradually increases with decreasing *L*, reaching 1.7 at $L = 1.8$. The higher concentration of heavy ions at lower *L*-values is expected because the scale heights of He^+ and O^+ are shorter than those for H^+ [see, for example, *Horwitz et al*., 1990, Figure 9].

[21] As described earlier, we often see during afternoon hours a gradual decline in the FLR frequency, or equivalently a rising level of mass density, but not until we examined a large number of days were we able to verify the statistical significance of this trend. Figure 8 shows, for each hourly bin at four selected *L*-values, the median value, the first quartile, and the third quartile in the distribution of the equatorial mass density. At all these *L*-values, the mass density stays relatively steady in the morning hours between 0700 and 1200 LT, and it rises in the afternoon with a different

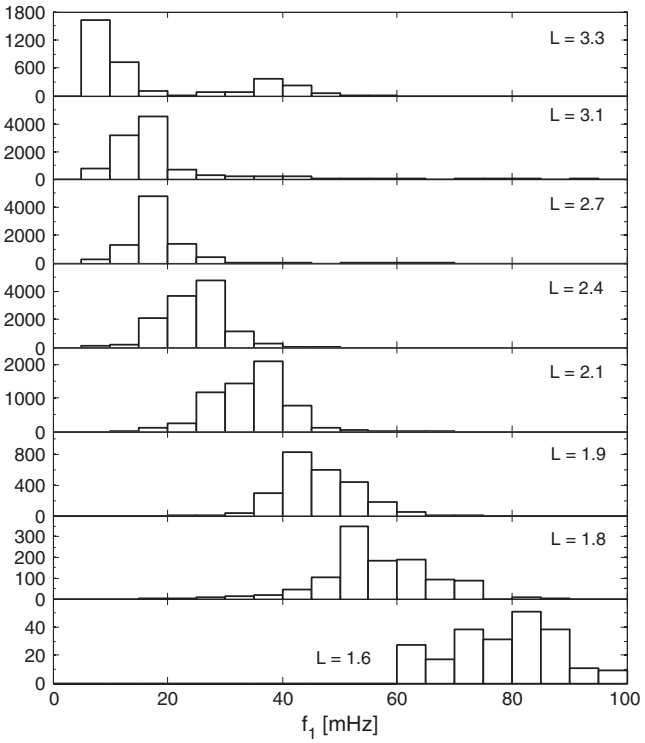

Figure 6. Histograms of FLR frequencies observed by McMAC station pairs.

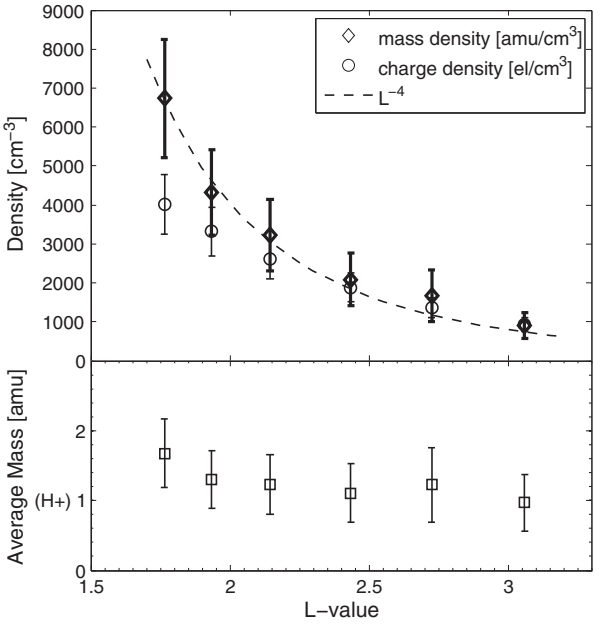

Figure 7. (top) The equatorial plasma mass density as inferred from observations of field line resonance, and the equatorial charge density as suggested by the RPI model of the plasmasphere. (bottom) Average ion mass as the ratio between the mass density and the charge density shown in the upper panel.

level of enhancement at each L-value. At $L = 2.1$ and 2.7, the afternoon rise in mass density continues in evening hours when the maximum density is 2–3 times of the prenoon value. At $L = 1.8$, the local time dependence may not appear as strong, but there are not enough FLR events detected in late afternoon hours to reveal the density level. The density level at $L = 3.1$, on the other hand, rises only in the afternoon but reverses trend in the evening.

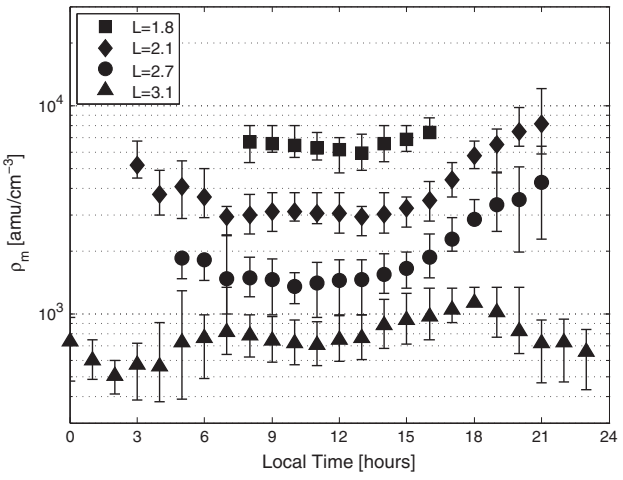

Figure 8. The local time dependence of plasma mass density as inferred by McMAC observations of field line resonance during July 2006 to June 2007. Symbols represent median values for each hourly bin, and each error bar spans between the first quartile and the third quartile.

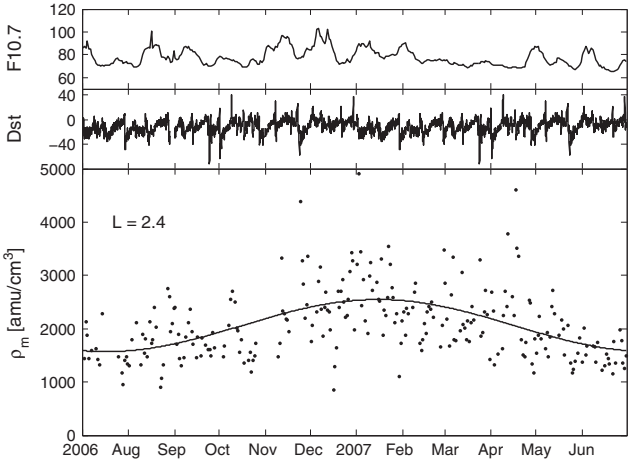

Figure 9. The solar radio flux $F_{10.7}$, the *Dst* index, and the daily equatorial mass density at $L = 2.4$ during July 2006 to June 2007. The curve in the bottom panel is a sine function fitted to the daily density values.

[22] Figure 9 shows the long-term variations in the equatorial mass density at $L = 2.4$, and the 10.7 cm solar radio flux $F_{10.7}$ (as a proxy for solar EUV radiation) and the *Dst* index for comparison. Previous work by *Vellante et al.* [2007] has demonstrated that the fundamental mode frequency f_1 at low L-shells is linearly proportional to $-F_{10.7}$ and that "anomalous" values of f_1 could occur during magnetic storms. Following *Vellante et al.* [2007], we also used the mean of the observations during 0900–1600 LT for daily density values, but we do not see a clear correlation between ρ_m and either $F_{10.7}$ or *Dst*. The two results are not necessarily contradictory, however. The interval studied by *Vellante et al.* [2007] is immediately after a solar maximum, whereas in our study the data were collected during a period of very low solar and geomagnetic activities. If we adopt the empirical relationship found by *Vellante et al.* [2007], the largest monthly variation in $F_{10.7}$ during the interval in our study only changes in f_1 by about 10% (or in ρ_m by 20%), a difference not easily discernible in Figure 9.

[23] On the other hand, the low solar and geomagnetic activity provided an opportunity to examine the annual variation of mass density that is visible in Figure 9. To assess the magnitude of the annual variation, we plot in the Figure a sine function determined by fitting the daily ρ_m values. The fitted sine function centered at 2059 amu/cm^3 is minimum at 1571 amu/cm^3 in July and maximum at 2547 amu/cm^3 in January. From the minimum to the maximum the density rises by 62%, an amount slightly higher than the increase of 21–44% found at $L = 1.6$–1.8 by *Vellante et al.* [2007].

5. Discussion

[24] Our statistical survey using one year of McMAC observations demonstrates not only many results in good agreement with previous studies but also a few surprises. The normalized distribution of FLR detection in Figure 5 confirms that FLR is mostly observed during daytime hours. Although FLR has been observed in the nightside magnetosphere [e.g., *Hughes et al.*, 1979], the occurrence of

nighttime FLR on the ground was little investigated. To our knowledge this study provides the first systematic survey of the infrequent nighttime FLR at low latitudes.

[25] The detection of FLR by the gradient method is inevitably tied to the signal to noise ratio and the amplitude of FLR which is a function of source strength and ionospheric damping. As the FLR frequencies examined in this study are mainly in the Pc 3–4 band, the upstream waves in the foreshock region are known to be an important energy source. In fact any variation in the solar wind dynamic pressure could also result in magnetopause perturbations, which in turn provide additional source energy. The compressional wave energy from these sources can travel to both dayside and nightside regions of the magnetosphere, coupling with the shear Alfvén wave that propagates along the field line. During daytime hours the high ionospheric conductivity sets a favorable stage for FLR excitation. During nighttime hours, the low ionospheric conductivity can either prevent the development of FLR or result in FLR with a lower Q and a greater resonance width [e.g., *Newton et al*., 1978; *Glassmeier et al*., 1984]. Detection of nighttime FLR by the gradient method, including the assessment of the optimal separation between ground stations, is an interesting subject that deserves further investigation.

[26] In our result the L-dependence of the equatorial mass density is inversely proportional to the flux tube volume, which has a slightly faster fall-off rate than that of the electron density (cf. Figure 7). The inferred average ion mass (M_i) gradually decreases from 1.7 at $L = 1.8$ to 1 at $L = 3.1$, but the difference may not be significant considering the possible overestimation in density at low L-values due to the adopted function for field-aligned density. The electron density for comparison is the most recent RPI empirical model of the plasmasphere that is valid for L-values ranging from 1.6 to 4 [*Ozhogin et al*., 2012]. Some other plasmaspheric electron density models, such as those developed by *Carpenter and Anderson* [1992] and by *Denton et al*. [2006], have lower fall-off rates of the electron density with respect to L and thus imply larger values in M_i at inner L-shells, but the use of those models for $L < 2.2$ would exceed the model limit. Our observations were made during a period of low solar and geomagnetic activities. In disturbed times there can be more heavy ions in the outer part of the plasmasphere, and the average ion mass can increase with L [*Berube et al*., 2005].

[27] We see an annual variation of the equatorial mass density in the plasmasphere that has also been seen in the electron density of the plasmasphere [e.g., *Carpenter*, 1962; *Carpenter and Anderson*, 1992], in the ionospheric density (see review by *Rishbeth and Müller-Wodarg* [2006]), and in the thermospheric neutral density [*Müller et al*., 2009]. Recently *Menk et al*. [2012] found that the annual variation of equatorial ion density at $L = 2.5$ is larger at American longitudes, where the asymmetry in solar illumination at conjugate ionospheres due to the configuration of the geomagnetic field is greatest. In the low-latitude topside ionosphere the electron density has a strong annual variation at all longitudes, despite longitudinal and latitudinal differences of this variation [e.g., *Su et al*., 1998]. The annual variation in thermospheric neutral density exists in both daytime and nighttime sectors [*Müller et al*., 2009], and the longitude effect remains to be investigated. It is conceivable that the annual variation in the thermosphere may translate to a similar variation in the ionosphere and possibly in the plasmasphere. Observations covering a wider region combined with modeling studies would help further understand this phenomenon.

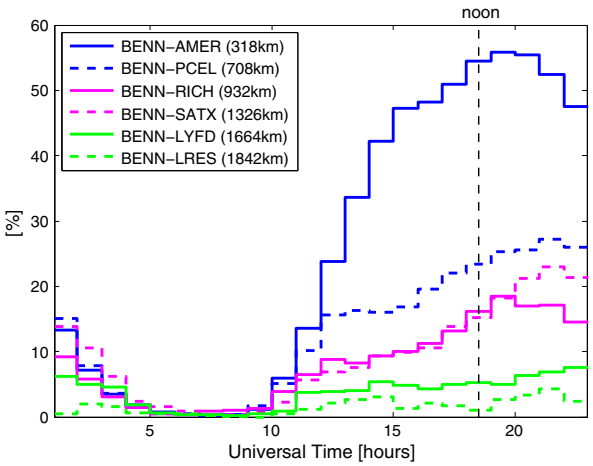

Figure 10. Normalized distribution of FLR detection observed by station pairs with different 48 distances of separation.

[28] This study presents a systematic study of the local time dependence of the plasmaspheric mass density inferred from FLR frequencies. Interestingly, none of the empirical plasmasphere models mentioned earlier indicates that the electron density is a function of local time, which means that, as a flux tube corotates with the Earth through different local time sectors, the replenishment or drainage of plasma by the underlying ionosphere has little effect on the electron density in the plasmasphere. In contrast, both physics models of the plasmasphere and event observations of middle- and low-latitude FLR suggest an increase in the plasma mass density during daytime hours. By using a physically realistic plasmasphere model, *Poulter et al*. [1984] showed that model eigenfrequencies of midlatitude field lines have a diurnal variation with maxima and minima at 0500 LT and 1800 LT, respectively. Observations of FLR events, such as in the study by *Chi et al*. [2000] using a pair of stations at $L = 2$, often find this gradual decline of FLR frequency due to the continuous outflow from the ionosphere during daytime hour. Using FLR observations at $L = 1.8$ and 2.8, *Waters et al*. [1994] also reported an early local morning increase in the plasma mass density, and they attributed the phenomenon to the heavy ion mass loading effects in the ionosphere around dawn. These processes of plasma supply from the ionosphere are expected to take place, but the ionization by solar radiation alone cannot readily explain our observations that (1) the density rise does not begin until noon, and (2) at certain L-values the density can continue to increase after dusk (cf. Figure 8).

[29] We should note that the high level of plasma mass density at dusk hours is not an artifact due to the quarter-wave modes resulting from the hemispheric asymmetry of the ionospheric conductivity [*Allan and Knox*, 1979]. We have seen in many daily plots a gradual decline of the FLR frequency from local noon to dusk (such as the example in Figure 4), which is different from the sharper transition between the quarter-wave and half-wave modes within 2 h of time as seen by *Obana et al*. [2008]. In addition, if the quarter-wave modes were important in our statistics, their

impact on density estimation would have been found at all L-values examined rather than at only $L = 2.1$ and 2.7 as shown in Figure 8. As the quarter-wave modes occur most likely around solstices and near the dawn and dusk terminators, we examined the local time distribution of FLR frequencies during the months close to equinoxes and found it to be statistically identical to that for the FLR frequencies for the entire year (not shown). In summary, the quarter-wave modes are not a statistical important part of the observed FLR frequencies in this study.

[30] On the other hand, the afternoon increase in plasma mass density resembles the distributions of thermospheric and ionospheric densities at low latitudes. Deriving the total mass density at 400 km altitude from CHAMP accelerometer measurements, *Liu et al*. [2005] discovered an anomalous distribution of thermospheric density that maximizes at about 20°–25° geomagnetic latitude on both sides of the equator between 10 and 20 magnetic local time. They also found that the electron density structure associated with the equatorial ionization anomaly extends from 10 MLT to postmidnight around 01 MLT, consistent with numerical modeling results [e.g., *Maruyama et al*., 2003]. These low-latitude density anomalies in the coupled thermosphere and ionosphere could result in a similar increase in plasmaspheric mass density in a limited range of L-shells between noon and midnight.

[31] We end this paper by noting a technical aspect of using ground-based magnetometers for FLR detection. It was a challenge to align all the nine McMAC magnetometers that span more than 2400 km on the same meridian, but the outcome is that our observations are essentially free from uncertainties due to local time separation. The good alignment also allows us to experiment with the separation distance and its impact on FLR detection. The appropriate separation should be comparable to the width of FLR, which depends on the Pedersen conductivity at the ionosphere and the radial gradient of the eigenfrequencies of field lines [e.g., *Mann et al*., 1995]. An additional consideration is that any two stations separated by a distance much less than 100 km should observe very similar waveforms because of the ionospheric screening effect [*Hughes and Southwood*, 1976]. Many studies have made successful FLR observations with a separation distance of ~100 km, but *Chi and Russell* [1998] also found that the gradient method could work for distances as long as 800 km. We compared the number of the FLR events detected by the Bennington-Americus pair with those by five other pairs with longer distances of separation. For the convenience in comparison Bennington is the northern station for all pairs. The results for the normalized distribution of FLR detection are plotted in Figure 10, which shows that the maximum rate of FLR detection dropped significantly when the separation in the north-south direction increased from 318 km to 708 km. Further increases in separation, however, only gradually reduced the maximum rate of detection. It was a surprise to us that the Bennington-Linares pair, with a separation of 1842 km, can still produce a detection rate of 5%. It is particularly interesting when we find that the Lyford-Linares pair with a shorter separation detected far fewer FLR events. We think that the stronger FLR amplitude observed by the station at higher latitude helps boost the signal to noise ratio in the cross-spectrum and enhance the detection rate. Large separations seem to work well for station pairs at low latitudes where the change in FLR frequency with respect to northward distance is gradual. A useful implication from this exercise is that one could allow larger separations between stations and construct more station pairs for FLR observations, enhancing the coverage of plasmaspheric sounding.

[32] **Acknowledgments.** We thank the engineers at UCLA and the hosts of McMAC stations for their hard work and support to make possible these geomagnetic observations. The Americus magnetometer station is hosted by William Jensen of Emporia State University. P.J.C. is grateful to Hermann Lühr for his comments about thermospheric observations. The McMAC project is sponsored by NSF grant ATM-0245139. M.B.M. was supported by NASA LWS grant NNX10AQ53G.

References

Allan, W., and F. B. Knox (1979), A dipole field model for axisymmetric Alfvén waves with finite ionospheric conductivities, *Planet. Space Sci.*, *27*, 79–85, doi:10.1016/0032-0633(79)90149-1.

Baransky, L. N., J. E. Borovkov, M. B. Gokhberg, S. M. Krylov, and V. A. Troitskaya (1985), High resolution method of direct measurement of the magnetic field lines' eigen frequencies, *Planet. Space Sci.*, *33*, 1369–1374.

Berube, D., M. B. Moldwin, and J. M. Weygand (2003), An automated method for the detection of field line resonance frequencies using ground magnetometer techniques, *J. Geophys. Res.*, *108*(A9), 1348, doi:10.1029/2002JA009737.

Berube, D., M. B. Moldwin, S. F. Fung, and J. L. Green (2005), A plasmaspheric mass density model and constraints on its heavy ion concentration, *J. Geophys. Res.*, *110*, A04212, doi:10.1029/2004JA010684.

Carpenter, D. L. (1962), Electron density variations in the magnetosphere deduced from whistler data, *J. Geophys. Res.*, *67*(9), 3345–3360, doi:10.1029/JZ067i009p03345.

Carpenter, D. L., and R. R. Anderson (1992), An ISEE/whistler model of equatorial electron density in the magnetosphere, *J. Geophys. Res.*, *97*(A2), 1097–1108.

Chen, L., and A. Hasegawa (1974), A theory of long-period magnetic pulsations, 1. Steady state excitation of field line resonance, *J. Geophys. Res.*, *79*(7), 1024.

Chi, P. J., and C. T. Russell (1998), An interpretation of the cross-phase spectrum of geomagnetic pulsations by the field line resonance theory, *Geophys. Res. Lett.*, *25*(24), 4445–4448.

Chi, P. J., C. T. Russell, and G. Le (1994), Pc 3 and Pc 4 activity during a long period of low interplanetary magnetic field cone angle as detected across the Institute of Geological Sciences array, *J. Geophys. Res.*, *99*(A6), 11127–11139.

Chi, P. J., C. T. Russell, S. Musman, W. K. Peterson, G. Le, V. Angelopoulos, G. D. Reeves, M. B. Moldwin, and F. K. Chun (2000), Plasmaspheric depletion and refilling associated with the September 25, 1998 magnetic storm observed by ground magnetometers at $L = 2$, *Geophys. Res. Lett.*, *27*(5), 633–636.

Chi, P. J., C. T. Russell, J. C. Foster, M. B. Moldwin, M. J. Engebretson, and I. R. Mann (2005), Density enhancement in plasmasphere-ionosphere plasma during the 2003 Halloween Superstorm: Observations along the 330th magnetic meridian in North America, *Geophys. Res. Lett.*, *32*, L03S07, doi:10.1029/2004GL021722.

Cummings, W. D., R. J. O'Sullivan, and P. J. Jr.Coleman (1969), Standing Alfvén waves in the magnetosphere, *J. Geophys. Res.*, *74*(3), 778–793.

Dent, Z. C., I. R. Mann, F. W. Menk, J. Goldstein, C. R. Wilford, M. A. Clilverd, and L. G. Ozeke (2003), A coordinated ground-based and IMAGE satellite study of quiet-time plasmaspheric density profiles, *Geophys. Res. Lett.*, *30*(12), 1600, doi:10.1029/2003GL016946.

Dent, Z. C., I. R. Mann, J. Goldstein, F. W. Menk, and L. G. Ozeke (2006), Plasmaspheric depletion, refilling, and plasmapause dynamics: A coordinated ground-based and IMAGE satellite study, *J. Geophys. Res.*, *111*, A03205, doi:10.1029/2005JA011046.

Denton, R. E., and D. L. Gallagher (2000), Determining the mass density along magnetic field lines from toroidal eigenfrequencies, *J. Geophys. Res.*, *105*(A12), 27717–27725.

Denton, R. E., K. Takahashi, I. A. Galkin, P. A. Nsumei, X. Huang, B. W. Reinisch, R. R. Anderson, M. K. Sleeper, and W. J. Hughes (2006), Distribution of densityalong magnetospheric field lines, *J. Geophys. Res.*, *111*, A04213, doi:10.1029/2005JA011414.

Dungey, J. W. (1954), Electrodynamics of the outer atmosphere, *Ionos. Res. Lab. Sci. Rep. 69*, Penn. State Univ., University Park.

Gallagher, D. L., P. D. Craven, and R. H. Comfort (2000), Global core plasma model, *J. Geophys. Res.*, *105*(A8), 18819–18833, doi:10.1029/1999JA000241.

Glassmeier, K. H., H. Volpers, and W. Baumjohann (1984), Ionospheric Joule dissipation as a damping mechanism for high latitude ULF pulsations: Observational evidence, *Planet. Space Sci.*, *32*(11), 1463–1466.

Grew, R. S., F. W. Menk, M. A. Clilverd, and B. R. Sandel (2007), Mass and electron densities in the inner magnetosphere during a prolonged disturbed interval, *Geophys. Res. Lett.*, *34*, L02108, doi:10.1029/2006GL028254.

Horwitz, J. L., R. H. Comfort, P. G. Richards, M. O. Chandler, C. R. Chappell, P. Anderson, W. B. Hanson, and L. H. Brace (1990), Plasmasphere-ionosphere coupling 2. Ion composition measurements at plasmaspheric and ionospheric altitudes and comparison with modeling results, *J. Geophys. Res.*, *95*(A6), 7949–7959.

Hughes, W. J., and D. J. Southwood (1976), An illustration of modification of geomagnetic pulsation structure by the ionosphere, *J. Geophys. Res.*, *81*(19), 3241–3247.

Hughes, W. J., R. L. McPherron, J. N. Barfield, and B. H. Mauk (1979), A compressional Pc4 pulsation observed by three satellites in geostationary orbit near local midnight, *Planet. Space Sci.*, *27*, 821–840.

Kawano, H., K. Yumoto, V. A. Pilipenko, Y.-M. Tanaka, S. Takasaki, M. Iizima, and M. Seto (2002), Using two ground stations to identify magnetospheric field line frequency as a continuous function of ground latitude, *J. Geophys. Res.*, *107*(A8), 1202, doi:10.1029/2001JA000274.

Kurchashov, Y. P., Y. S. Nikomarov, V. A. Pilipenko, and A. Best (1987), Field line resonance effects in local meridional structure of mid-latitude geomagnetic pulsations, *Ann. Geophys., Ser.A*, *5*, 147–154.

Liu, H., H. Lühr, V. Henize, and W. Köhler (2005), Global distribution of the thermospheric total mass density derived from CHAMP, *J. Geophys. Res.*, *110*, A04301, doi:10.1029/2004JA010741.

Mann, I. R., A. N. Wright, and P. S. Cally (1995), Coupling of magnetospheric cavity modes to field line resonances: A study of resonance widths, *J. Geophys. Res.*, *100*(A10), 19441–19456.

Maruyama, N., S. Watanabe, and T. J. Fuller-Rowell (2003), Dynamic and energetic coupling in the equatorial ionosphere and thermosphere, *J. Geophys. Res.*, *108*(A11), 1396, doi:10.1029/2002JA009599.

Menk, F. W., D. Orr, M. A. Clilverd, A. J. Smith, C. L. Waters, D. K. Milling, and B. J. Fraser (1999), Monitoring spatial and temporal variations in the dayside plasmasphere using geomagnetic field line resonances, *J. Geophys. Res.*, *104*(A9), 19955.

Menk, F. W., I. R. Mann, A. J. Smith, C. L. Waters, M. A. Clilverd, and D. K. Milling (2004), Monitoring the plasmapause using geomagnetic field line resonances, *J. Geophys. Res.*, *109*, A04216, doi:10.1029/2003JA010097.

Menk, F. W., S. T. Ables, R. S. Grew, M. A. Clilverd, and B. R. Sandel (2012), The annual and longitudinal variations in plasmaspheric ion density, *J. Geophys. Res.*, *117*, A03215, doi:10.1029/2011JA017071.

Milling, D. K., I. R. Mann, and F. W. Menk (2001), Diagnosing the plasmapause with a network of closely spaced ground-based magnetometers, *Geophys. Res. Lett.*, *28*(1), 115–118.

Müller, S., H. Lühr, and S. Rentz (2009), Solar and magnetospheric forcing of the low latitude thermospheric mass density as observed by CHAMP, *Ann. Geophys.*, *27*, 2087–2099.

Newton, R. S., D. J. Southwood, and W. J. Hughes (1978), Damping of geomagnetic pulsations by the ionosphere, *Planet. Space Sci.*, *26*, 201–209.

Obana, Y., F. W. Menk, M. D. Sciffer, and C. L. Waters (2008), Quarter-wave modes of standing Alfvén waves detected by cross-phase analysis, *J. Geophys. Res.*, *113*, A08203, doi:10.1029/2007JA012917.

Obana, Y., G. Murakami, I. Yoshikawa, I. R. Mann, P. J. Chi, and M. B. Moldwin (2010), Conjunction study of plasmapause location using ground-based magnetometers, IMAGE-EUV, and Kaguya-TEX data, *J. Geophys. Res.*, *115*, A06208, doi:10.1029/2009JA014704.

Obayashi, T., and J. A. Jacobs (1958), Geomagnetic pulsations and the Earth's outer atmosphere, *Geophys. J. Roy. Astron. Soc.*, *1*(1), 53–63.

Ozhogin, P., J. Tu, P. Song, and B. W. Reinisch (2012), Field-aligned distribution of the plasmaspheric electron density: An empirical model derived from the IMAGE RPI measurements, *J. Geophys. Res.*, *117*, A06225, doi:10.1029/2011JA017330.

Pilipenko, V. A., and E. N. Fedorov (1994), Magnetotelluric sounding of the crust and hydrodynamic monitoring of the magnetosphere with the use of ULF waves, in *Solar Wind Sources of Magnetospheric Ultra-Low-Frequency Waves, Geophys. Monogr. Ser., 81*, edited by M. J. Engebretson, K. Takahashi, and M. Scholer, pp. 283–292, AGU, Washington, D. C.

Poulter, E. M., W. Allan, G. J. Bailey, and R. J. Moffett (1984), On the diurnal period variation of mid-latitude ULF pulsations, *Planet. Space Sci.*, *32*(6), 727–734.

Reinisch, B. W. *et al.* (2000), The Radio Plasma Imager investigation on the IMAGE spacecraft, *Space Sci. Rev.*, *91*, 319–359, doi:10.1023/A:1005252602159.

Rishbeth, H., and I. C. F. Müller-Wodarg (2006), Why is there more ionosphere in January than in July? The annual asymmetry in the F2-layer, *Ann. Geophys.*, *24*, 3293–3311, doi:10.5194/angeo-24-3293-2006.

Russell, C. T., P. J. Chi, V. Angelopoulos, W. Goedecke, F. K. Chun, G. Le, M. B. Moldwin, and E. G. Reeves (1999), Comparison of three techniques for locating a resonating magnetic field line, *J. Atmos. Solar-Terr. Phys.*, *61*, 1289–97.

Russell, C. T., P. J. Chi, D. J. Dearborn, Y. S. Ge, B. Kuo-Tiong, J. D. Means, D. R. Pierce, K. M. Rowe, and R. C. Snare (2008), THEMIS ground-based magnetometers, *Space Sci. Rev.*, *141*(1–4), 389–412, doi:10.1007/s11214-008-9337-0.

Samson, J. C. (1972), Three-dimensional polarization characteristics of high-latitude Pc5 geomagnetic micropulsations, *J. Geophys. Res.*, *77*(31), 6145–6160.

Sheeley, B., M. Moldwin, H. Rassoul, and R. Anderson (2001), An empirical plasmaspheric and trough density model: CRRES observations, *J. Geophys. Res.*, *106*(A11), 25631–25641, doi:10.1029/2000JA000286.

Southwood, D. J. (1974), Some features of field line resonances in the magnetosphere, *Planet. Space Sci.*, *22*, 483–491.

Su, Y. Z., G. J. Bailey, and K.-I. Oyama (1998), Annual and seasonal variations in the low-latitude topside ionosphere, *Ann. Geophys.*, *16*, 974–985.

Takahashi, K., R. E. Denton, R. R. Anderson, and W. J. Hughes (2004), Frequencies of standing Alfvén wave harmonics and their implication for plasma mass distribution along geomagnetic field lines: Statistical analysis of CRRES data, *J. Geophys. Res.*, *109*, A08202, doi:10.1029/2003JA010345.

Tamao, T. (1966), Transmission and coupling resonance of hydromagnetic disturbances in the non-uniform Earth's magnetosphere, *Sci. Rep. Tohoku Univ., Ser. 5*, *17*(43).

Troitskaya, V. A. (1994), Discoveries of Sources of Pc 2–4 waves-A review of research in the former USSR, in *Solar Wind Sources of Magnetospheric Ultra-Low-Frequency Waves*, edited by M. J. Engebretson, K. Takahashi, and M. Scholer, American Geophysical Union, Washington, D.C., doi:10.1029/GM081p0045.

Vellante, M., and M. Förster (2006), Inference of the magnetospheric plasma mass density from field line resonances: A test using a plasmasphere model, *J. Geophys. Res.*, *111*, A11204, doi:10.1029/2005JA011588.

Vellante, M., M. De Lauretis, M. Förster, S. Lepidi, B. Zieger, U. Villante, V. A. Pilipenko, and B. Zolesi (2002), Geomagnetic field line resonances at low latitudes: Pulsation event study of 16 August 1993, *J. Geophys. Res.*, *107*(A5), 1060, doi:10.1029/2001JA900123.

Vellante, M., M. Förster, U. Villante, T. L. Zhang, and W. Magnes (2007), Solar activity dependence of geomagnetic field line resonance frequencies at low latitudes, *J. Geophys. Res.*, *112*, A02205, doi:10.1029/2006JA011909.

Waters, C. L. (2000), ULF resonance structure in the magnetosphere, *Adv. Space Res.*, *25*(7/8), 1541–1558.

Waters, C. L., F. W. Menk, and B. J. Fraser (1991), The resonance structure of low latitude Pc3 geomagnetic pulsations, *Geophys. Res. Lett.*, *18*(12), 2293–2296.

Waters, C. L., F. W. Menk, and B. J. Fraser (1994), Low latitude geomagnetic field line resonance: Experiment and modeling, *J. Geophys. Res.*, *99*(A9), 17547–17588.

Webb, D. C., L. J. Lanzerotti, and C. G. Park (1977), A comparison of ULF and VLF measurements of magnetospheric cold plasma densities, *J. Geophys. Res.*, *82*(32), 5063–5072.